Optics Letters

Continuously wavelength-tunable high harmonic generation via soliton dynamics

Francesco Tani,[1,*] Michael H. Frosz,[1] John C. Travers,[1,2] and Philip St.J. Russell[1,3]

[1]Max Planck Institute for the Science of Light, Staudtstr. 2, 91058 Erlangen, Germany
[2]School of Engineering and Physical Sciences, Heriot-Watt University, Edinburgh, EH14 4AS, UK
[3]Department of Physics, University Erlangen–Nuremberg, Erlangen, Germany
*Corresponding author: francesco.tani@mpl.mpg.de

Received 6 March 2017; revised 9 April 2017; accepted 10 April 2017; posted 10 April 2017 (Doc. ID 287968); published 24 April 2017

We report the generation of high harmonics in a gas jet pumped by pulses self-compressed in a He-filled hollow-core photonic crystal fiber through the soliton effect. The gas jet is placed directly at the fiber output. As the energy increases, the ionization-induced soliton blueshift is transferred to the high harmonics, leading to emission bands that are continuously tunable from 17 to 45 eV.

OCIS codes: (320.7120) Ultrafast phenomena; (190.2620) Harmonic generation and mixing; (320.5520) Pulse compression; (260.7200) Ultraviolet, extreme.

https://doi.org/10.1364/OL.42.001768

Soliton dynamics offers a range of powerful tools for nonlinear manipulation of ultrashort light pulses. In gas-filled hollow-core photonic crystal fiber (HC-PCF), the weak anomalous dispersion gives access to this dynamics over a broad spectral range in the visible and near-infrared regions. Moreover, the pressure-tunable dispersion adds an additional degree for controlling the interplay between linear and nonlinear effects [1]. In addition to the Kerr effect, temporally nonlocal nonlinearities, such as Raman scattering and ionization offer additional tools for manipulating guided light pulses [2–4]. By making the use of these dynamics, gas–filled HC-PCFs have been successfully exploited for supercontinuum generation, efficient generation of broadband ultraviolet and vacuum ultraviolet radiation, and soliton self-compression down to sub-single cycle durations [5–7], an ideal pump source for high harmonic generation (HHG) [8,9].

HHG is an extreme nonlinear process, which depends on many parameters, such as the peak intensity, the duration and the global phase of the driving pulse, as well as the phase-matching conditions. By controlling these parameters, it is possible to manipulate the spectrum of the emitted extreme ultraviolet (XUV) radiation, and perhaps even the temporal profile of the associated attosecond pulses [10–13]. Manipulation of high harmonic spectra has been achieved previously by exploiting various different mechanisms, such as controlling the temporal chirp of the driving laser, the ionization-induced blueshift of the driver pulse in the generating medium [2,10,13], and tuning the central wavelength of the driver using an optical parametric amplifier [14]. Here we combine a gas-filled HC-PCF with a gas–jet for HHG driven by laser pulses of a few tens of microjoules, which undergo soliton self-compression in the fiber. We show that by exploiting the interaction of the soliton with the ionization current in the waveguide we can continuously upshift the soliton frequency [4,15,16] and, as a result, tune the frequency of the generated harmonics, achieving in this way almost 3 eV of blueshift, larger than reported in previous work (1–2 eV) [2,10] while, at the same time, compressing the driving pulse. The high efficiency and low pulse energies suggest that this HHG scheme will pave the way to the development of a tunable XUV source that can easily be scaled to megahertz repetition rates. (Soliton self-compression in gas-filled HC-PCF was previously demonstrated at 38 MHz repetition rate [17].)

In the experiment, pulses of durations of 25 fs at 800 nm (1.5 eV) with 1 kHz repetition rate and energies in the range 10–56 μJ (Femtolasers FEMTOPOWER PRO HE CEP) were launched into a 26 cm long kagomé-style hollow-core PCF with a 46 μm core diameter (Fig. 1), using an achromatic lens with a 20 cm focal length. The pulse energy was varied using a half–wave plate and a thin-film polarizer. The dispersion introduced by the optics was pre-compensated for by a pair of chirped mirrors providing −250 fs^2 per bounce and further adjusted by tuning the laser grating compressor. One end of the fiber was enclosed in a gas cell filled with 5 bar of He, while the other was fed into a vacuum chamber which, because of the

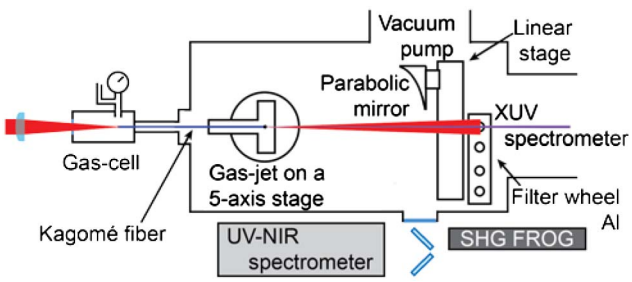

Fig. 1. Sketch showing the experimental arrangement.

small fiber core, could be evacuated down to 10^{-5} mbar using a turbo-molecular pump with a pumping speed of 250 l/s [18].

At the output, the fiber was precisely positioned perpendicular to a pulsed gas jet emitted from a nozzle 200 μm in diameter. Two 200 nm thick aluminum filters were placed on the other side of the jet, aligned so as to face the fiber endface, and the spectrum of the isolated HHG beam was measured using a flat-field spectrometer (Dr. Hoerlein & Partner). The pulsed gas jet was placed on a five-axis stage, making it possible to adjust the position of the nozzle with respect to the fiber endface. It was supplied with Ar gas at 5 bar using a piezo valve that was synchronized with the laser pulses and the CCD camera of the XUV spectrometer. The distance between the fiber axis and the nozzle was ~270 μm, and the pressure in the jet was estimated (following [19]) to be ~100 mbar. When the gas jet was operating, the pressure in the vacuum chamber rose to a few times 10^{-3} mbar, resulting in ~20% absorption of the XUV radiation before the detector, which was 1.2 m from the gas jet. A mirror was inserted after the fiber and before the aluminum filters, so as to deliver the beam through a 3.3 mm CaF_2 viewport outside the vacuum chamber for diagnostic tests of the fundamental laser pulse after propagation through the fiber. This mirror was also used to maximize the coupling of the pump beam into the fundamental mode of the fiber, achieving in this way ~84% transmission which, considering the 2 dB/m fiber loss at 800 nm, translates to ~94% launch efficiency. We could launch over 70 μJ into the core without damage. When damage did occur at higher energies, this was mainly caused by beam-pointing instabilities in the laser. Note that the launch efficiency did not degrade when we filled the gas cell with 5 bar of He, since the nonlinearity of this gas is very low and the ionization potential very high.

The pulse dynamics in the fiber depends strongly on the He filling pressure, which was selected so that the pulses were propagating in the anomalous dispersion regime with soliton order $N = \sqrt{\gamma P_0 T_0^2/|\beta_2|}$ between 2 and ~5 (depending on the launched pump energy), where γ is the nonlinear coefficient, P_0 is the soliton peak power, T_0 is the soliton duration, and β_2 is the group velocity dispersion. Under these conditions, for constant pressure along the fiber, the pump pulse experiences clean adiabatic soliton self-compression as it propagates, with a compression factor inversely proportional to N [1]. The length over which the input laser pulse compresses is proportional to L_d/N, where $L_d = T_0^2/\beta_2$ is the dispersion length. In the presence of a pressure gradient, self-compression occurs over a longer distance. In both cases, the compression length can be adjusted to match precisely the fiber length, without strongly affecting the final pulse duration, by adding a positive chirp to the input pulse. In the experiment, we match the two lengths by positively chirping the pulses launched in the fiber by ~200 fs^2. As the energy increases, the pulse gets shorter, its peak intensity rises, and the influence of ionization becomes more important, eventually causing the self-compressing pulse to blueshift in frequency. The magnitude of this shift is given by [10,20]

$$\delta\omega = \frac{e^2 L}{2cn_0 m_e \epsilon_0 \omega}\frac{\partial N_e}{\partial t},$$

where c is the speed of light, m_e is the electron mass, ϵ_0 is the vacuum permittivity, e is the electronic charge, and L is the width of the plasma. The equation shows that the shift is proportional to L and to the slope of the free electron density $\partial N_e/\partial t$, so it is larger for shorter pulses. As a result of the long interaction length over which a short pulse duration is sustained, a very large frequency shift can be achieved through self-compression. The dynamics is described by the plots in Fig. 2, which show the temporal and spectral evolution of a 25 fs pulse with 50 μJ of energy and a 210 fs^2 positive chirp, as it propagates along the fiber. The simulations were based on a unidirectional field equation [21], including photoionization with the ADK model [22]. They predict that for these parameters the pulse should compress down to sub-3 fs. The lower plots show snapshots of the pulse together with the relative free electron density. As the pulse compresses, the free electron density increases and, when it becomes high enough (at ~20 cm), the pulse accelerates and blueshifts.

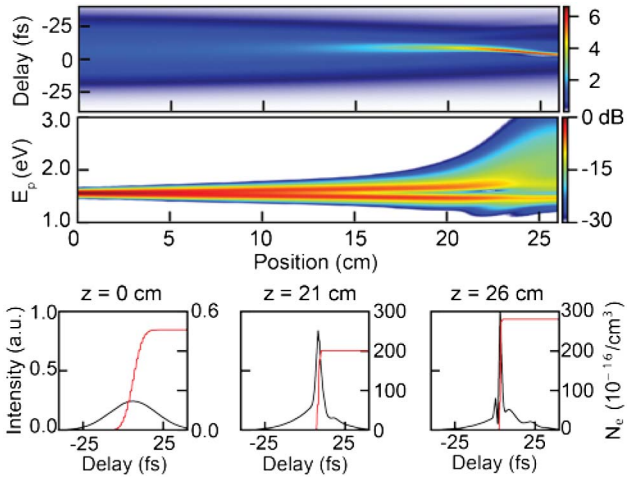

Fig. 2. Temporal and spectral evolution of a 25 fs pulse with 50 μJ of energy and positively chirped by 210 fs^2 undergoing soliton self-compression in a HC-PCF filled at the input with 5 bar of He. Snapshots of the pulse and the corresponding free electron densities (simulation).

The resulting compressed pulses have sufficient intensity to generate high harmonics in the gas–jet and, because the jet is placed after the fiber endface, short trajectories are favored. In the experiment, the nozzle was placed as close as possible to the fiber endface so as to maintain constant pulse peak intensity over the width of the gas jet. (The Rayleigh length was estimated to be ~1.3 mm.) Figure 3 plots the pulse spectra at the output of the fiber (left), together with the high harmonic spectra (right) for increasing pump pulse energy. The driver pulse spectra were measured with the gas–jet switched off, confirming that the pulse blueshifts as it propagates along the gas-filled fiber. The harmonic spectra were integrated along the spatial axis of the CCD. The bandwidth of each harmonic grows with increasing pulse energy, suggesting temporal compression of the driving pulses. Along with spectral broadening, there is a clear correlation between the pump pulse spectra and the high harmonic spectra: the harmonic frequencies track the blueshifting soliton driver as the input energy is increased.

The harmonics do not follow the average wavelength of the pulses launched into the PCF (ν_{pump}), but rather the central wavelength of the blueshifting soliton (ν_{sol}). This indicates that

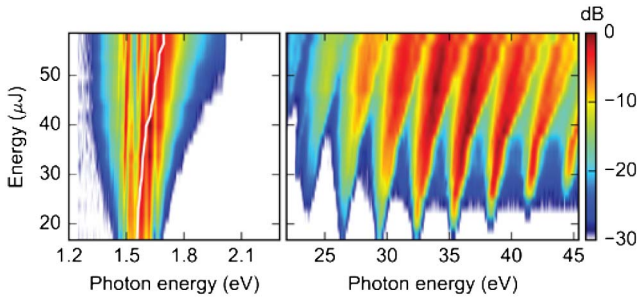

Fig. 3. Measured pump pulse (left) and high-harmonic (right) spectra for increasing launched pulse energy. The white curve on the left-hand side tracks the frequency of the 17th harmonic divided by 17.

the generation of the high-order harmonics is predominantly driven by the self-compressing blueshifting pulse, which contains most of the energy. To highlight this, a white curve, representing the average frequency of the 17th harmonic divided by its harmonic order ($\nu_{17}/17$), is drawn on top of the pump pulse spectra [Fig. 3 (left)]. This curve clearly follows the frequency of the blueshifting soliton. Further support is evident in the right-hand plot of Fig. 4, where $\nu_{17}/17$ clearly does not follow ν_{pump}, but rather ν_{sol} (red dots), which was obtained from spectrograms measured at different energies (see below). The shift to a higher frequency is the same for all the harmonics, as shown in the left-hand plot in 4, and amounts to more than 100% of the adjacent harmonic spacing, permitting the harmonic spectra to be tuned continuously from at least 17–45 eV.

For pump energies below ∼25 μJ, a few harmonics are generated, and only a weak spectral broadening can be observed. As the energy in the fiber is increased up to ∼40 μJ, the harmonics are generated more efficiently, and the spectra start to broaden asymmetrically to the high-frequency side. However, at these energies, the compression length exceeds the fiber length, and highly chirped pulses are delivered to the gas–jet, resulting in a frequency shift of the harmonics, in agreement with the observations reported in [12]. For higher energies, the two lengths become comparable and the self-compressing pulses blueshift within the fiber because of the gas–ionization, resulting in a much more pronounced frequency shift and spectral broadening of the harmonics. The right-hand plot in Fig. 4 shows the central wavelength of the pump pulse for increasing energy, the corresponding frequency shift of the 17th harmonic (which becomes much more marked for energies above 40 μJ), and the soliton central frequency, which agrees perfectly with the harmonic frequency shift.

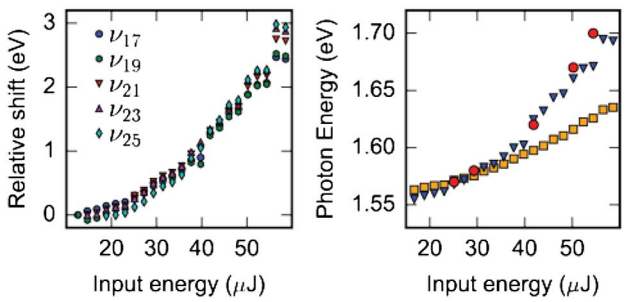

Fig. 4. Frequency shifts of the 17th–25th harmonics relative to the frequency at the lowest input energy, plotted as a function of pump energy (left). The plot on the right panel shows the central frequency of the pump pulse (squares), the averaged frequency of the 17th harmonic divided by 17 (triangles), and the soliton central frequency (circles) obtained from the measured spectrograms.

The dynamics is further confirmed by the reconstructed spectrograms shown in Fig. 5, which were obtained from frequency resolved optical gating (FROG) traces measured using a home-built second harmonic (SH) FROG with a 10 μm thick BBO crystal. The FROG was placed outside the vacuum chamber, and the traces in Fig. 5 correspond to launching pulses with 29 and 50 μJ energy into the fiber. In the reconstruction of the spectrograms, we compensated for the dispersion introduced by the vacuum chamber window (3.3 mm CaF_2), the air path (1.4 m), and the half-wave plate (840 μm SiO_2 + 675 μm CaF_2), and used a 10 fs (FWHM) Gaussian pulse as the spectrogram gate function. After compensation, we obtained respectively ∼38 and ∼15 fs. The pulse compression is limited mainly by a band of fiber loss at ∼2 eV (∼625 nm), which also causes the sharp cutoff in the pump spectrum for energies above ∼45 μJ. This loss band introduces a local change in dispersion that affects the soliton dynamics, limiting the final pulse duration. The details of this process will be published elsewhere. Note that the time direction ambiguity of the SH FROG is removed by the knowledge of the dispersive elements placed before the temporal characterization.

Following the procedure reported in [23], we estimate the conversion efficiency to the 23rd harmonic to be $\sim 10^{-8}$, taking into account the diffraction efficiency of the grating, the quantum efficiency of the CCD and the spectral transmission of the Al filter. We expect that the conversion efficiency can be greatly increased by optimizing the nozzle design and the

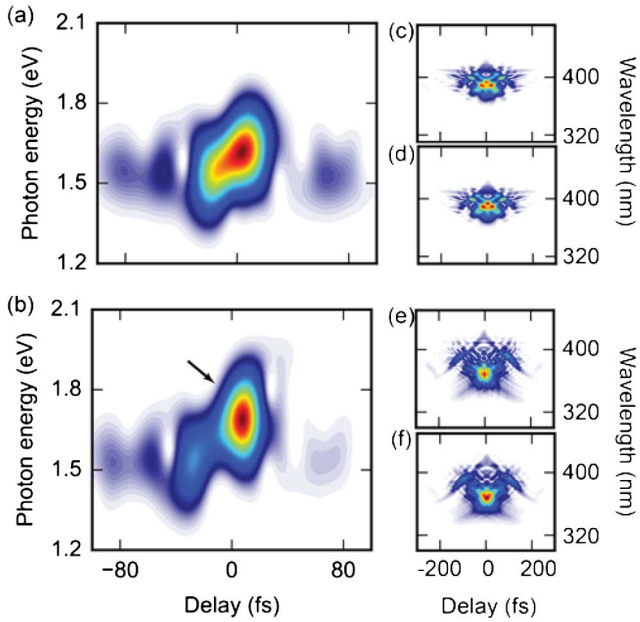

Fig. 5. Reconstructed spectrogram for (a) 29 and (b) 50 μJ launched pulse energy. (c) Measured and (d) retrieved FROG traces at the fiber output for 29 μJ of pulse energy. (e) and (f) Same for 50 μJ of pulse energy. A linear scale is used for all the plots. The black arrow indicates the blueshifting pulse.

pressure in the gas jet, so as to improve phase-matching to the high-harmonics.

In agreement with the discussion above, when a 29 μJ pulse is launched in the fiber, the output spectrogram [Fig. 5(a)] reveals a strongly chirped pulse while, in the 50 μJ case, the spectrogram clearly shows that most of the energy is carried by a blueshifting pulse with a minor chirp, only a small fraction remaining at ∼1.51 eV (∼810 nm). This confirms that the high harmonics must be predominantly generated by the blueshifting pulse. According to our measurements the frequency shift of the higher-order harmonics is a consequence of the soliton blueshift in the fiber. We saw no evidence of ionization in the Ar jet, an observation that is supported by numerical simulations (not shown). For higher peak intensities, however, ionization-related effects in the jet may become more important and give rise to an even larger blueshift.

In conclusion, high harmonics can be generated in an Ar gas jet using pump pulses self-compressed by soliton effects in gas–filled HC-PCF. In previous work [2,10–12], frequency tuning of the harmonics was achieved by exploiting the ionization of the generating medium or by chirping the pump pulse. In both cases, the generation and tuning of the harmonics were strongly coupled to each other. In contrast, soliton dynamics in the presence of ionization in gas-filled HC-PCF permits the frequency of the pump pulse to be upshifted before HHG, resulting in an independent continuous tuning of the high harmonics over a frequency range greater than the spacing between neighboring harmonic orders. Finally, we note that pump pulse durations, much shorter than the ∼15 fs achieved in the experiments, could be reached by modifying the fiber design so as to shift the loss band to a shorter wavelength.

REFERENCES

1. J. C. Travers, W. Chang, J. Nold, N. Y. Joly, and P. St.J. Russell, J. Opt. Soc. Am. B **28**, A11 (2011).
2. C. A. Froud, E. T. Rogers, D. C. Hanna, W. S. Brocklesby, M. Praeger, A. M. de Paula, J. J. Baumberg, and G. J. Frey, Opt. Lett. **31**, 374 (2006).
3. F. Belli, A. Abdolvand, W. Chang, J. C. Travers, and P. St.J. Russell, Optica **2**, 292 (2015).
4. W. Chang, P. Hölzer, J. C. Travers, and P. St.J. Russell, Opt. Lett. **38**, 16 (2013).
5. T. Balciunas, C. Fourcade-Dutin, G. Fan, T. Witting, A. A. Voronin, A. M. Zheltikov, F. Gerome, G. G. Paulus, A. Baltuska, and F. Benabid, Nat. Commun **6**, 6117 (2015).
6. P. St.J. Russell, P. Hölzer, W. Chang, A. Abdolvand, and J. C. Travers, Nat. Photonics **8**, 278 (2014).
7. A. Ermolov, K. F. Mak, M. H. Frosz, J. C. Travers, and P. St.J. Russell, Phys. Rev. A **92**, 3 (2015).
8. O. H. Heckl, C. J. Saraceno, C. R. E. Baer, T. Südmeyer, Y. Y. Wang, Y. Cheng, F. Benabid, and U. Keller, Appl. Phys. B **97**, 369 (2009).
9. G. Fan, T. Balciunas, S. Hässler, C. F. Dutin, T. Witting, A. Voronin, A. Zheltikov, F. Gérôme, G. Paulus, and A. Baltuska, in *Conference on Lasers and Electro-Optics (CLEO): Science and Innovations* (2015), paper SM1P–1.
10. C. Altucci, T. Starczewski, E. Mevel, C.-G. Wahlström, B. Carré, and A. L'Huillier, J. Opt. Soc. Am. B **13**, 148 (1996).
11. Z. Chang, A. Rundquist, H. Wang, I. Christov, H. C. Kapteyn, and M. M. Murnane, Phys. Rev. A **58**, R30 (1998).
12. D. G. Lee, J.-H. Kim, K.-H. Hong, and C. H. Nam, Phys. Rev. Lett. **87**, 243902 (2001).
13. C. Winterfeldt, C. Spielmann, and G. Gerber, Rev. Mod. Phys. **80**, 117 (2008).
14. B. Shan, A. Cavalieri, and Z. Chang, Appl. Phys. B **74**, S1 (2002).
15. E. E. Serebryannikov and A. M. Zheltikov, Phys. Rev. A **76**, 013820 (2007).
16. P. Hölzer, W. Chang, J. C. Travers, A. Nazarkin, J. Nold, N. Y. Joly, M. F. Saleh, F. Biancalana, and P. St.J. Russell, Phys. Rev. **107**, 203901 (2011).
17. K. F. Mak, M. Seidel, O. Pronin, M. H. Frosz, A. Abdolvand, V. Pervak, A. Apolonski, F. Krausz, J. C. Travers, and P. St.J. Russell, Opt. Lett. **40**, 1238 (2015).
18. A. Ermolov, K. F. Mak, F. Tani, P. Hölzer, J. C. Travers, and P. St.J. Russell, Appl. Phys. Lett. **103**, 261115 (2013).
19. H. Pauly, *Atom, Molecule, and Cluster Beams I* (Springer, 2000), Vol. **28**.
20. S. C. Rae and K. Burnett, Phys. Rev. A **46**, 2 (1992).
21. W. Chang, A. Nazarkin, J. C. Travers, J. Nold, N. Y. Joly, and P. St.J. Russell, Opt. Express **19**, 21018 (2011).
22. A. M. Ammosov, N. B. Delone, and V. P. Krainov, Sov. Phys. JETP **64**, 1191 (1986).
23. S. Hädrich, K. Klenke, J. Rothhardt, M. Krebs, A. Hoffmann, O. Pronin, V. Pervak, J. Limpert, and A. Tünnermann, Nat. Photonics **8**, 779 (2014).